

Geochemistry of Rare-Earth Elements in the Surface Bottom Sediments of the Northwestern Pacific

V.V. Sattarova , K.I. Aksentov

*V.I. Il'ichev Pacific Oceanological Institute, Far Eastern Branch of the Russian Academy of Sciences,
ul. Baltiiskaya 43, Vladivostok, 690041, Russia*

Received 12 July 2017; accepted 18 December 2017

Abstract—The distribution and fractionation of rare-earth elements (REE) in the Northwestern Pacific surface sediments are studied. The REE contents in the sediments were 30–106 ppm, and the Y contents ranged from 9.34 to 24.5 ppm. The bottom sediments located near the Kuril–Kamchatka arc were depleted in REE as compared with the sediments of the abyssal plain of the Pacific, the Kuril basin of the Sea of Okhotsk, and the northwestern Bering Sea. The effect of distributive provinces and lithodynamic setting on the REE composition and REE contents in the sediments was expressed as a positive correlation of the LREE/HREE ratio with the grain composition, Rb/Sr, and Nb/Y and its negative correlation with Zr/Rb. The variations in the bulk REE composition were due to the variations in LREE contents.

Keywords: rare-earth elements, bottom sediments, Kuril Basin, Sea of Okhotsk, Bering Sea, Pacific

INTRODUCTION


Rare-earth elements (REE) represents a group of elements with the unique geochemical characteristics determined by their chemical properties and characterized by an 4f- electron configurations (Henderson, 1984). Three-valent lanthanides behave like coherent elements in geochemical processes, while cerium (Ce) and europium (Eu) naturally change their oxidation degrees to 4⁺ and 2⁺, respectively. These unique properties of Ce and Eu compared to their neighboring elements allow using them as sensitive geochemical indicators for paleoclimatic and paleogeographical reconstructions of bottom sediments (Dou et al., 2010).

The REE behavior in sea and oceanic sediments have been many times analyzed in the publications of Soviet, Russian and foreign researchers (Balashov, 1976; Li, 1982; Dubinin and Volkov, 1986; Murray et al., 1991; Bailey, 1993; Otsuka et al., 2000; Baturin and Yushina, 2007; Akagi et al., 2011; Dubinin et al., 2013; Sattarova et al., 2014; Sattarova and Artemova, 2015; Zou et al., 2015; Aksentov and Sattarova, 2016; etc.). REE geochemistry has been studied as at field test sites as using the seismic profile method applied to different oceanic facial zones (Toyoda et al., 1990; Dubinin, 1994, 1998a; Strekopytov and Dubinin, 1996; Dubinin and Sval'nov, 2001, 2003; etc.). It has been demonstrated that the further into the pelagic zone, the higher the REE accumulation in oceanic sediments compared to the coastal terrigenous deposits. This is due to sorption (es-

pecially light ones) of REE from oceanic water by clayey minerals and hydrogenous iron/manganese oxyhydroxides whose proportion increase in the pelagic zone (Volkov and Fomina, 1973; Gurvich et al., 1980). REE composition in the clayey sediments of continental periphery, in general, is close to REE composition in shales (North American shale rock NASC, PAAS, etc.) but relatively depleted in heavy lanthanides (Dubinin, 2006; Taylor and McLennan, 1985).

In the international water of the Pacific, deep-water bottom sediments with high REE content were found. In these areas of the Pacific, REE concentration is higher than in many continental deposits, as those being developed in China (Kato et al., 2011).

The REE content in the sediments Far Eastern seas have been rarely studied. These studies include an investigation into REE content and fractioning in the deep-sea cores obtained from the Yamato Basin in the Sea of Japan (Murray et al., 1991). The authors considered the effect of sediments lithology and diagenetic processes on REE composition. The lanthanides migration and accumulation was determined by lithodynamic processes, mainly by the mineralogical composition of distributive provinces in the sediments from the Amur Gulf of the Sea of Japan (Aksentov and Sattarova, 2016). The bottom sediments at the Academy of Sciences Plateau in the Sea of Okhotsk have a significant positive Ce anomaly, which is related to Fe–Mn oxides formation (Zou et al., 2015). In the Bering Sea REE distribution in the pore water and suspension was investigated (Akagi et al., 2011; Soyol-Erdene and Huh, 2013). In (Anikiev et al., 1997) the authors considered the distribution and sedimentation flows of different chemical elements including REE in the bottom sediments from the Gulf of Anadyr (Bering Sea).

 Corresponding author.

E-mail address: sv_8005@mail.ru (V.V. Sattarova)

In this study we try to trace REE and yttrium distribution in the bottom sediments of the Western Pacific and consider the interrelation between lanthanides and grain composition, organic matter and other chemical elements.

STUDY AREAS

Kuril Basin of the Sea of Okhotsk. The maximum depth of the Kuril Basin reaches 3521 m. Located in the south of the Sea of Okhotsk it is regarded as one of the back-arc basins (Mazarovich, 2011). It has a triangular-shape reducing to the north. Its relief is an abyssal plane delineated along its isobathic line at 3000 m (Rodnikov et al., 2005). In its southwestern part it has a developed sedimentary cover, whose thickness varies from 4000 to 7000 m. The basin formed under stretching conditions from the early Oligocene to the late Miocene; and it started to deepen in the early Pliocene (Mazarovich, 2011). The basin's sedimentary deposits can be subdivided into two units. The upper one is an interlayering of turbidities and volcanogenic sediments (ashes) and covers the Miocene–Quaternary stratigraphic interval. The lower one is formed by pelagic clays and mudstones with rare interlayers of volcanic materials. As for its age, it can be regarded as Cretaceous–Paleogene, considering the sedimentation rate (Rodnikov et al., 2005).

Northwestern Pacific. On the oceanic side of the Kuril–Kamchatka Trench at the very edge of the Pacific bed there is a flat plateau known as the Zenkevich swell. Its height is only 200–400 m above the adhering oceanic bottom at the width of 180–250 miles. In the southeast, the swell's surface gradually becomes transitions to the seafloor. Above the swell's dome laying at the depth of 5000–5500 m rise a number of hills (100–300 m) and a number of high mountains reaching the depths of 1700–1900 m. The falls and rises of the swell's surface are oriented transversely to its strike (Belousov and Udintsev, 1981). The Kuril–Kamchatka Trench's slope is mainly composed of strongly weathered pillow lavas of plagioclase and pyroxene–plagioclase basalts. Apart from the basalts its composition includes sedimentary clayey–siliceous and sandstone rocks; metamorphosed sedimentary and volcanogenic rocks (Vasil'ev et al., 1986). This region is susceptible to active volcanic activity (Bezrukov, 1955; Udintsev, 1955). The terrigenous and pyroclastic material coming from the neighboring areas mix with the organic matter in suspensions. Another factor affecting sedimentation in the area is the Kuril–Kamchatka stream bringing mainly Bering Sea waters. The depth of the Kamchatka straits is crucial for water-exchange conditions between the northwestern part of the Pacific and the Sea of Okhotsk (Rogachev and Verkhunov, 1995).

Bering Sea. The biggest of the Russian Far East seas is subdivided from the Pacific by the chain of the Aleutian Islands and their western extension—the Commander Islands. The sea's maximum depth does not exceed 4420 m, which is equal to the average depth of the Pacific (Lisytsyn, 1966),

and it lies at the boundary of the ice and temperate zones. The external slope of the Aleutian arc has multiple benches and terraces. The Bering Sea can be divided into two areas: to the south lies the Orbuhev Seamount being a wide underwater surface of 4000 m along its isobathic line, whose heights reach 3500 m. Its sedimentary thickness changes from 1000 to 2000 m. According to A.P. Lisytsyn (1966), these are sediments of different kinds including terrigenous, biogenic, volcanogenic and mixed kinds. The most typical biogenic sediments include diatomic and spicule siliceous ones. The large areas are covered with the gravel and pebbles brought by ices and accumulated at different depths. The southern offshore is typically covered by the volcanogenic sediments represented by rough and fine aleuritic silts. The neighboring Pacific brings in foraminiferal sediments and covers large areas with siliceous and sponge sands. The continental slopes of the Bering Sea are mainly covered with large siltstones and their lower parts—by fine siltstones and silts-shale silts (mostly terrigenous ones). In some places, there are sand concentrations and stripes as well as the gravel-cobble sediments marking bedrock exposures.

MATERIALS AND METHODS

In this study we analyzed the surface sediments obtained during scientific expeditions on the board of research vessels “Sonne” (So223, 2012) “Akademik M.A. Lavrent'ev” (LV55, 2011 г.; LV63, 2013 г.; LV71, 2015) (Fig. 1). Table 1 summarizes the coordinates of the sampling sites and the mass percentage of grain size fractions in the sediments.

The grain size was measured using the ANALYSETTE 22 particle size analyzer (Fritsch, Germany) following the well-mastered technique (Botsul, 2002).

The total organic carbon (C_{org}) content was detected using the TOC-VCPN analyzer with the SSM-5000A solid sample combustion unit (SHIMADZU, Japan). The relative standard deviation for the total carbon was 1.5%, and for nonorganic carbon—2.0%.

Bulk chemical analysis of the samples was performed in the Common Use Center of the Far East Geological Institute of the Russian Academy of Sciences. To perform lithochemical analyses, selected samples were first dried in a dewatering box at the temperature of 30–50 °C until they became air-dried. Then the samples underwent open acid decomposition. The REE content was detected using the ICP-MS technique with the Agilent 7500c mass-spectrometer (Agilent Technologies, USA) and ^{115}In as an internal standard (at finite concentration $10^{-7}\%$). The concentration of other elements was determined using the ICP-AES technique with the iCAP 6500Duo spectrometer (Thermo Electron Corporation, USA) and cadmium solution as an internal standard (concentration 10–4%). The detection accuracy was confirmed using State Standard Reference Sample analyses such as OOPE 402 (siliceous silt), OOPE 201 (terrigenous volcanic silt).

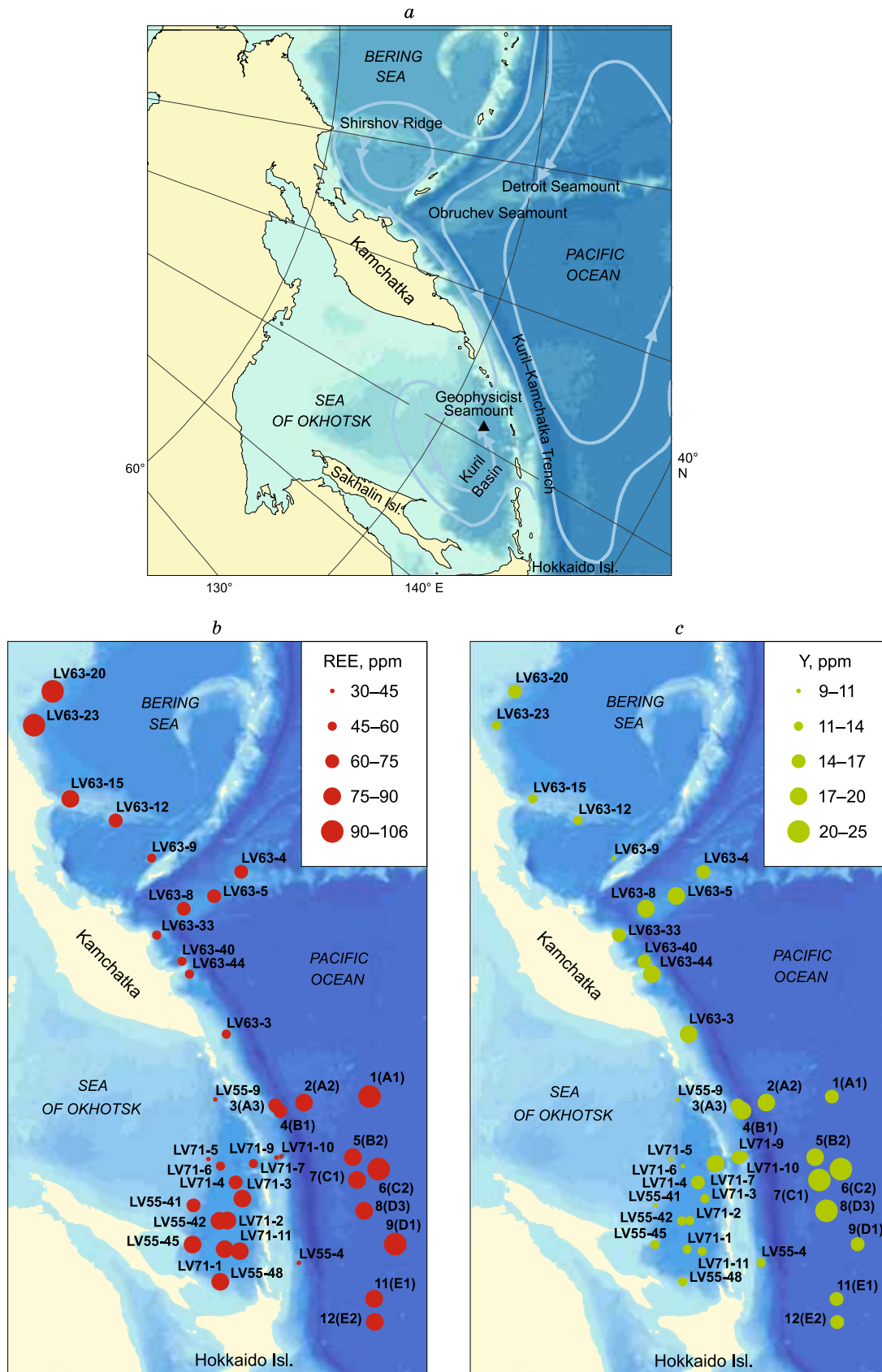


Fig. 1. Map of study area and location of bottom sediment sampling stations. The arrows indicate a schematic circulation systems.

Table 1. Geographic location, water depth and grain composition of surface sediment samples from the Northwestern Pacific

Stations	Coordinates		Depth, m	Content of grain fractions, %		
	Lat N	Long E		> 0.063 mm	0.004–0.063 mm	< 0.004 mm
Kuril Basin (Sea of Okhotsk)						
LV71-1	46°08.8'	146°00.0'	3481	0	46	54
LV71-2	46°41.08'	147°27.99'	3352	0	53	47
LV71-3	46°38.002'	148°59.995'	3363	0	46	54
LV71-4	47°12.005'	149°36.992'	3366	0	67	33
LV71-5	48°37.261'	150°00.315'	1700	0	71	29
LV71-6	48°02.960'	150°00.292'	3351	2	55	43
LV71-7	46°57.020'	151°5.011'	3300	4	65	31
LV71-11	45°36.300'	146°23.100'	3206	0	44	56
LV55-9	49°31.255'	153.27.141'	1937	0	78	21
LV55-41	48°9.488'	147°8.372'	1639	0	49	51
LV55-42	46°56.91'	147°12.289'	3354	0	43	57
LV55-45	47°18.395'	145°10.358'	2426	0	78	21
LV55-48	45°33.14'	144°19.964'	767	0	55	45
Northwestern Pacific						
LV55-4	43°24.743'	147°36.978'	2909	1	76	24
LV71-9	46°16.086'	152°02.101'	3430	2	74	24
LV71-10	46°07.870'	152°12.182'	4722	0	71	29
1(A1)	43°58.190'	157°19.796'	5412	0	68	31
2(A2)	46°14.024'	155°33.100'	4869	0	67	33
3(A3)	47°14.261'	154°42.319'	4976	1	78	21
4(B1)	46°58.001'	154°32.703'	5767	0	57	43
5(B2)	43°34.990'	153°57.964'	5378	8	67	25
6(C2)	42°29.002'	153°59.905'	5297	1	71	28
7(C1)	43°02.217'	152°59.129'	5222	1	77	22
8(D3)	42°14.614'	151°43.506'	5127	0	76	24
9(D1)	40°35.012'	150°59.630'	5401	0	63	37
11(E1)	40°12.891'	148°06.042'	5349	0	67	33
12(E2)	39°43.417'	147°10.014'	5229	0	72	28
LV63-3	50°12.6995	157°28.5013	1495	46	37	17
LV63-4	51°37.5235	167°49.7646	2951	11	63	26
LV63-5	52°29.0948	165°49.9814	3131	21	56	23
LV63-8	53°33.9217	164°27.5782	3083	22	52	26
LV63-33	54°20.0411	162°07.1840	1465	14	58	28
LV63-40	52°59.2205	160°56.5172	2927	34	43	22
LV63-44	52°30.9397	160°16.9615	1668	2	62	37
Bering Sea						
LV63-9	55°23.0315	167°24.9123	2560	3	71	26
LV63-12	57°11.0513	169°40.2556	1888	0	73	27
LV63-15	59°14.3871	170°46.4688	794	67	20	14
LV63-20	60°23.1146	179°47.2203	1125	3	78	20
LV63-23	61°08.9513	176°45.6812	1891	3	74	23

REE results are usually presented as normalized on the North American Shale Composite (NASC) (Gromet et al., 1984) to exclude the effect of different REE prevalence. The values of Eu and Ce fractioning were calculated according to the following formulas:

$$Eu_{an} = 2 \times Eu/Eu^N / (Sm/Sm^N + Gd/Gd^N);$$

$Ce_{an} = 2 \times Ce/Ce^N / (La/La^N + Nd/Nd^N)$, respectively (Dubinin, 2006).

The light/heavy REE ratio was considered as:

$$LREE/HREE = (La/La^N + 2 \times Pr/Pr^N + Nd/Nd^N) / (Er/Er^N + Tm/Tm^N + Yb/Yb^N + Lu/Lu^N).$$

This formula is based on a large number of elements and less to the influence of analysis errors in the determination of individual lanthanides.

The obtained element database was processed using the statistical methods of correlation and cluster analysis. Since the initial concentrations have different scales, they were standardized through z-transformation. In this study, the Ward's method of cluster analysis was used. Euclidean distance (expressed in arbitrary units) was used as a measure of similarity (affinity). The cluster analysis was performed following the Q-technique, which allowed us to group sampling stations with similar geochemical parameters. For the cluster analysis, only element composition data were considered, which, in our opinion, was a more correct approach to determination of the sedimentations' geochemical types.

RESULTS

The total concentrations of REE and yttrium in the studied bottom sediments are presented in Fig. 1. In the whole, one can see three zones of maximum REE concentration: the north-western part of the Bering Sea (stations LV63-20, LV63-23); the abyssal plane of the Pacific (stations 1(A1), 6(C2), 9(D1)); and the deep part of the Kuril Basin of the Sea of Okhotsk (stations LV71-1, LV71-2, LV55-48). The areal distribution of yttrium demonstrates another pattern. Now, let's consider each particular area.

Kuril Basin of the Sea of Okhotsk. Based on grain composition, sediments from the Kuril Basin are represented by clayey-silt and silty-clay ooze of olive color with a high concentration of diatoms. Surface sediments within the interval of 1–6 cm include liquid and semiliquid silts.

The organic carbon values varies between 0.84–1.92%, 1.45% in average; the silicon ranges from 26.15 to 31.20%, 28.82% in average (Table 2). Compared to sediments from the Bering Sea and the Northwestern Pacific, Kuril Basin sediments are rich in manganese (1.29% in average), lithium (29.2 ppm), cesium (3.63 ppm), thorium (4.05 ppm), lead (18.63 ppm) and rubidium (53.86 ppm).

The total REE concentration in the surface sediments varies from 30.08 ppm (station LV55-9) to 89.58 ppm (station LV55-48), 68.98 ppm in average. The yttrium concentration ranges from 9.34 ppm (station LV71-5) to 18.65 ppm (station LV71-7), 12.49 ppm in average. It should be noted that the total concentration of lanthanides varies within 30.08–89.58 ppm (Table 3) with insignificant positive Eu and Ce anomalies. Analysis of REE distribution patterns in the sediments allowed us to separate the last into two groups. The first group includes bottom sediments with relatively homogeneous REE distribution in which light REE prevail, and the second includes stations with the prevalence of heavy REE (Fig. 2a, b).

Northwestern Pacific. The grain composition of the sediments from the stations located in the abyssal plane adjacent to the Kuril–Kamchatka Trench includes silty clay and

clayey silt ooze of light and dark brown colors. These are semiliquid, viscous and plastic silts (Sattarova and Artemova, 2015). The stations located along Kamchatka are represented by terrigenous and terrigenous–diatom sediments of gray-green color with sandy silt and silty sand and sand-silt-clay structures. Sediments from the Obruchev and Detroit Seamounts are terrigenous, sand-silt-clay and light brown with insignificant inclusions of diatoms and carbonates.

The studied sediments contain maximum average amount of aluminum (6.12%), iron (3.62%), calcium (2.88%), magnesium (1.44%), scandium (15.34 ppm), strontium (277 ppm) and zirconium (79.6 ppm). The C_{org} varies from 0.44 to 1.55%, 0.97% in average; the silicon ranges from 21.95 to 31.84%, 28.02% in average (Table 2).

The total REE concentration varies from 40.3 ppm at station LV55-4 to 105.4 ppm at station 9(D1) (Table 3), 70.90 ppm in average; the yttrium concentration—ranges from 12.57 ppm (station LV55-4) to 24.50 ppm (station 7(C1)), 17.06 ppm in average. NASC-normalized, REE showed a similar distribution (Fig. 2c–f) with the noticeable prevalence of heavy REE over light ones (LREE/HREE varies from 0.43 to 0.93) (Table 3). In sediments from some stations, a positive Eu anomaly ($Eu_{an} = 0.95–1.32$) was observed, and the Ce anomaly values varies with the range of 0.80–1.15.

Bering Sea. The bottom sediments of the Bering Sea are soft and their color changes from gray green to dark gray. Based on the grain composition the sediments are classified clayey silt, the only exception is a sample from station LV63-15 that has a sandy structure. The studied sediments are of terrigenous type with insignificant inclusions of diatoms, their pieces, and sponge spicules.

The sediments from the Bering Sea contain maximum average concentrations of organic carbon (1.54%), silicon (30.91%), titanium (0.31%), potassium (1.48%), niobium (5.22 ppm), chrome (74.06 ppm), and zinc (100.4 ppm).

The total concentration of REE in the samples varies from 46.29 ppm (station LV63-9) to 98.06 ppm (station LV63-20), 77.44 ppm in average; the yttrium concentration—ranges from 10.85 ppm to 14.15 ppm, 13.10 ppm in general.

Considering the distribution of the NASC-normalized REE it can be noticed that it is generally flat with an insignificant rise in the domain of middle and heavy rare-earth elements (Fig. 2e). These spectra are somewhat similar to ones from the Northwestern Pacific but have a more expressed Eu anomaly. Almost all the stations demonstrated insignificant Ce deficiency ($Ce_{an} = 0.90–0.94$). Three stations (LV63-15, LV63-20, LV63-23) showed insignificant increase of light rare-earth elements (LREE/HREE > 1).

DISCUSSIONS

The grain composition is one of the key factors that determine rare-earth fractioning in sediments (Zhang et al., 2012), so increase of fine fractions increases the total REE

Table 2. Chemical composition of the sediments from the Northwestern Pacific

Station	Element																					
	wt. %							ppm														
	C _{org}	Si	Al	Fe	Mn	Ca	Ti	Mg	K	Li	Nb	Cs	Cr	Hf	Th	U	Sc	Pb	Rb	Sr	Zn	Zr
Kuril Basin (Sea of Okhotsk)																						
LV71-1	1.92	26.86	4.83	3.04	1.75	0.75	0.23	1.31	1.54	28.94	5.47	4.71	48.25	1.42	4.84	1.33	9.41	22.53	68.16	201	109.3	54.05
LV71-2	1.56	29.11	5.30	3.45	0.30	0.72	0.24	1.31	1.65	31.38	5.51	5.21	47.08	1.52	4.87	1.22	10.57	18.73	73.35	160	119.2	57.38
LV71-3	1.45	29.29	4.95	3.29	0.25	1.01	0.23	1.34	1.43	26.75	4.48	4.39	39.67	1.41	4.10	1.06	11.11	20.73	59.46	167	119.9	53.93
LV71-4	1.18	27.99	4.86	3.39	3.12	1.48	0.25	1.27	1.11	36.16	3.48	3.21	30.88	1.38	2.99	1.35	13.76	16.28	44.37	207	105.8	49.89
LV71-5	1.34	30.79	3.52	2.35	0.35	1.53	0.17	1.12	0.90	14.54	2.15	1.98	24.24	0.93	1.97	0.86	9.21	16.12	28.48	195	88.9	38.10
LV71-6	1.24	27.68	3.47	2.41	3.87	1.14	0.18	1.23	0.99	48.88	2.60	2.44	24.27	1.05	2.39	1.42	9.40	16.02	34.34	208	102.5	41.87
LV71-7	0.84	27.47	5.50	4.03	1.69	2.44	0.30	1.41	0.89	29.57	2.04	1.94	20.13	2.94	1.75	0.82	19.58	14.58	26.07	244	94.9	52.30
LV71-11	1.83	26.15	4.48	2.87	2.60	0.74	0.22	1.22	1.56	29.21	6.45	4.54	48.07	1.68	5.82	2.16	9.55	25.08	66.57	208	95.9	55.33
LV55-9	1.38	31.20	3.70	2.37	0.04	1.99	0.18	1.03	0.72	9.81	1.22	1.12	20.43	1.00	1.32	0.99	11.10	9.66	17.35	215	53.8	38.97
LV55-41	1.40	30.30	4.45	2.96	0.50	0.75	0.21	1.15	1.40	26.95	4.65	3.83	41.21	1.35	4.76	1.31	10.23	23.06	58.66	185	125	52.75
LV55-42	1.75	28.05	4.73	3.07	2.12	0.71	0.23	1.21	1.56	38.64	5.39	4.71	47.11	1.49	5.64	1.57	10.60	22.48	70.60	201	112.6	59.59
LV55-45	1.67	30.42	4.83	2.96	0.18	0.68	0.24	0.99	1.60	27.02	5.82	3.97	44.96	1.48	5.59	1.46	9.15	16.49	69.80	186	68.9	53.07
LV55-48	1.28	29.37	5.30	3.59	0.06	0.75	0.25	1.09	1.77	31.74	6.78	5.07	52.62	1.75	6.57	1.59	10.07	20.45	83.00	187	74.7	63.03
Mean	1.45	28.82	4.61	3.06	1.29	1.13	0.23	1.21	1.32	29.20	4.31	3.63	37.61	1.49	4.05	1.32	11.06	18.63	53.86	197	97.80	51.56
St. dev.	0.30	1.59	0.67	0.50	1.31	0.57	0.04	0.13	0.35	9.76	1.83	1.35	11.91	0.50	1.76	0.36	2.84	4.27	21.22	22	21.45	7.62
Northwestern Pacific																						
LV55-4	1.34	31.08	3.52	2.15	0.10	2.03	0.17	0.99	0.73	10.65	1.88	1.57	17.62	1.17	1.68	0.98	9.84	12.43	20.91	175	66.73	43.43
LV71-9	1.55	28.68	6.20	4.35	0.13	3.15	0.34	1.44	0.80	12.19	1.69	1.33	23.70	1.68	1.42	0.69	21.74	9.52	19.14	262	78.9	56.11
LV71-10	0.95	28.99	4.86	3.37	0.25	1.84	0.26	1.35	1.00	15.77	3.21	1.76	28.32	1.33	1.90	0.99	15.73	12.32	25.87	208	76.2	53.39
1(A1)	0.81	28.58	5.90	3.31	0.39	1.38	0.26	1.38	1.31	23.00	4.30	4.15	34.10	2.11	4.44	1.28	13.20	25.20	51.30	239	86.30	87.00
2(A2)	0.81	28.69	5.97	3.75	0.36	1.59	0.31	1.50	1.28	24.20	3.92	3.91	37.30	2.15	4.32	1.39	16.50	22.60	50.60	259	99.70	92.20
3(A3)	1.55	28.34	5.38	3.60	0.15	1.83	0.30	1.58	1.09	22.00	2.86	2.70	37.00	1.77	2.76	1.32	13.70	13.80	36.50	231	83.70	71.00
4(B1)	0.98	27.33	6.99	4.97	0.19	3.07	0.42	1.89	1.08	18.90	2.82	2.52	37.10	1.81	2.74	1.09	18.30	14.10	34.50	295	88.20	73.60
5(B2)	0.78	28.86	5.84	3.12	0.30	1.56	0.25	1.24	1.25	21.40	4.23	4.05	24.10	2.25	4.41	1.32	13.50	24.00	47.40	247	79.40	96.00
6(C2)	0.69	27.73	6.38	3.18	0.32	1.65	0.27	1.28	1.40	22.60	4.59	4.74	27.70	2.42	5.05	1.30	13.40	26.90	55.00	245	80.50	101.00
7(C1)	0.44	31.84	6.57	2.46	0.21	1.67	0.19	0.75	1.17	18.10	3.74	3.29	13.70	3.02	3.73	1.21	9.87	19.80	36.50	239	73.10	119.00
8(D3)	0.58	30.25	6.41	2.64	0.28	1.94	0.22	0.89	1.21	18.70	3.86	3.65	9.80	2.89	3.87	1.26	11.20	20.40	39.00	236	73.80	110.00
9(D1)	1.36	27.09	5.95	3.36	0.95	0.97	0.27	1.39	1.63	39.80	5.90	6.13	43.70	1.97	6.80	1.75	14.00	34.60	74.20	206	121.20	94.60
11(E1)	1.45	26.20	5.11	3.05	1.02	0.94	0.24	1.32	1.35	35.80	5.09	4.85	32.40	1.79	5.39	1.68	11.70	27.90	60.90	192	117.00	76.20
12(E2)	1.40	28.65	5.20	3.12	0.60	1.00	0.24	1.27	1.31	28.60	5.21	4.79	38.30	1.91	5.37	1.69	11.90	27.30	59.90	188	93.60	79.00
LV63-3	0.79	27.65	7.98	5.37	0.10	4.32	0.43	1.73	1.05	13.74	2.11	1.82	48.93	1.88	1.47	0.73	23.21	6.73	27.25	339	94.79	68.39
LV63-4	0.79	21.95	5.02	2.86	0.15	10.86	0.25	1.18	1.13	16.23	2.85	1.94	29.61	1.65	2.21	0.82	11.64	12.75	30.03	566	74.87	66.41
LV63-5	0.57	24.92	6.68	3.63	0.23	7.62	0.33	1.44	1.19	16.19	2.81	1.69	39.95	2.03	2.11	0.77	15.86	10.47	29.36	451	86.74	84.49
LV63-8	0.57	28.97	7.20	4.00	0.22	3.53	0.38	1.59	1.37	17.52	3.49	1.77	48.56	2.26	2.35	0.88	16.66	10.21	33.72	333	93.39	92.17
LV63-33	1.06	27.41	7.46	4.77	0.07	3.27	0.40	2.11	1.36	23.65	2.67	1.83	91.54	1.83	1.78	0.88	20.33	7.25	31.81	303	94.96	69.65
LV63-40	1.54	27.74	6.16	3.94	0.06	2.47	0.35	1.86	1.33	23.53	2.84	1.97	64.08	1.77	1.92	1.13	17.58	7.98	33.17	264	102.89	67.10
LV63-44	0.93	27.43	7.79	4.93	0.08	3.88	0.42	1.92	1.19	17.43	2.30	1.54	73.98	1.80	1.43	0.78	22.18	6.86	26.86	331	96.22	68.87
Mean	0.97	28.02	6.12	3.62	0.29	2.88	0.30	1.44	1.20	20.95	3.45	2.95	38.17	1.98	3.20	1.14	15.34	16.82	39.23	277	88.68	79.60
St. dev.	0.37	2.07	1.07	0.87	0.26	2.38	0.08	0.34	0.20	7.12	1.14	1.42	19.53	0.44	1.60	0.32	4.03	8.39	14.60	92	14.03	18.92
Bering Sea																						
LV63-9	1.69	29.80	5.79	3.19	0.04	2.23	0.28	1.60	1.16	19.33	2.55	1.57	64.17	1.68	1.03	1.56	12.87	6.22	28.40	307	97.53	62.83
LV63-12	1.92	29.71	5.44	3.17	0.04	1.72	0.29	1.39	1.42	28.38	5.05	3.38	72.73	3.81	1.62	1.70	12.72	9.22	52.34	230	132.92	67.49
LV63-15	0.70	31.83	6.45	3.46	0.04	1.91	0.33	1.16	1.76	24.37	5.22	2.55	91.70	3.44	1.11	1.57	12.55	8.30	55.19	291	73.53	59.61
LV63-20	1.65	31.62	5.59	2.99	0.04	2.00	0.33	1.29	1.54	23.33	6.72	2.75	70.64	5.06	1.78	1.47	11.98	10.41	56.66	225	99.28	57.16
LV63-23	1.76	31.58	5.29	2.89	0.03	1.92	0.31	1.26	1.52	24.68	6.55	3.00	71.08	5.09	1.83	1.37	11.46	9.56	58.91	229	98.68	54.84
Mean	1.54	30.91	5.71	3.14	0.04	1.96	0.31	1.34	1.48	24.02	5.22	2.65	74.06	3.82	1.47	1.53	12.32	8.74	50.30	256	100.4	60.38
St. dev.	0.48	1.06	0.45	0.22	0.01	0.18	0.02	0.17	0.22	3.24	1.67	0.68	10.38	1.40	0.38	0.12	0.59	1.60	12.47	39	21.17	4.95

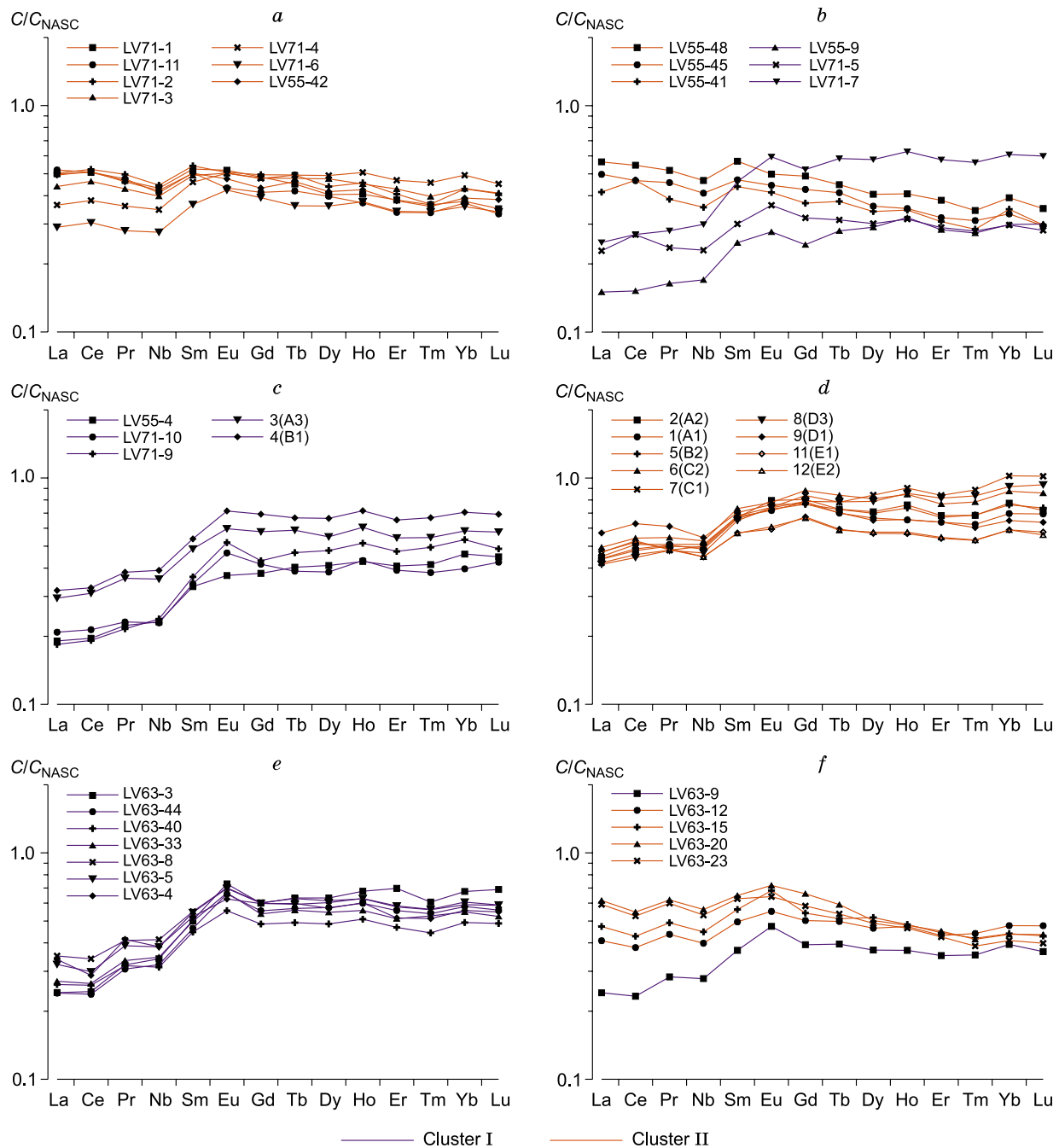


Fig. 2. NASC-normalized REE distribution patterns. *a, b*, The bottom sediments of the Kuril Basin of the Sea of Okhotsk; *c–e*, the bottom sediments of the Northwestern Pacific; *f*, the bottom sediments of the Bering Sea.

concentration in the sediments (Fig. 1*b*, Table 3). When considering REE distribution it should be noted that sediments with coarse fraction have a negative Ce anomaly in their composition, which becomes positive in fine fractions (Fig. 2). According to (Tlig and Steinberg, 1982) coarse fractions being mainly amorphous silica are in deficiency of cerium and light rare earth. According to A.V. Dubinin (2006) the clayey material of pelagic sediments, and oceanic and sea terrigenous sediments are often enriched by light

REE with no anomalous Ce behavior. Figure 3 demonstrates the features of the REE fractionation in the sediments of the Northwestern Pacific. Here LREE/HREE correlates with the geochemical, biogenic and lithological parameter. The effect of the distributive provinces can be traced in the negative Zr/Rb dependence being an indicator of heavy mineral content, and in positive Nb/Y indicating acid pyroclastics. Microscopic analysis demonstrated the presence of volcanic glass. Explosive eruptions in Holocene–late Pleistocene are

Table 3. REE concentration in the bottom sediments of the Northwestern Pacific, ppm

Station	La	Ce	Pr	Nd	Sm	Eu	Gd	Tb	Dy	Ho	Er	Tm	Yb	Lu	$\Sigma P3D$	Y	Eu _{an}	Ce _{an}	LREE/ HREE
Kuril Basin (Sea of Okhotsk)																			
LV71-1	15.99	37.01	3.68	14.23	2.99	0.64	2.52	0.38	2.10	0.42	1.30	0.18	1.17	0.17	82.80	12.49	1.03	1.09	1.26
LV71-2	16.12	38.16	3.92	14.67	3.09	0.63	2.57	0.42	2.28	0.47	1.38	0.18	1.33	0.20	85.43	12.73	0.98	1.10	1.21
LV71-3	14.06	33.76	3.39	13.13	2.80	0.62	2.49	0.41	2.47	0.47	1.46	0.20	1.33	0.20	76.78	13.16	1.04	1.10	1.02
LV71-4	11.64	27.80	2.85	11.45	2.62	0.62	2.48	0.42	2.55	0.53	1.59	0.23	1.53	0.22	66.52	14.60	1.07	1.07	0.77
LV71-5	7.31	19.66	1.86	7.59	1.71	0.45	1.66	0.27	1.57	0.33	0.98	0.14	0.92	0.14	44.59	9.34	1.17	1.18	0.81
LV71-6	9.28	22.19	2.21	9.10	2.09	0.52	2.04	0.31	1.87	0.39	1.16	0.17	1.11	0.16	52.61	10.84	1.12	1.07	0.82
LV71-7	7.96	19.71	2.21	9.86	2.64	0.74	2.72	0.50	3.01	0.65	1.96	0.28	1.88	0.29	54.41	18.65	1.21	0.99	0.47
LV71-11	16.63	37.06	3.75	13.60	2.87	0.54	2.15	0.36	2.07	0.39	1.15	0.17	1.15	0.16	82.04	12.26	0.94	1.09	1.37
LV55-9	4.81	11.09	1.30	5.61	1.41	0.34	1.26	0.24	1.51	0.33	0.96	0.14	0.93	0.14	30.08	10.09	1.13	0.95	0.56
LV55-41	13.29	34.21	3.05	11.74	2.50	0.51	1.93	0.32	1.77	0.36	1.05	0.14	1.08	0.14	72.10	10.77	1.02	1.22	1.25
LV55-42	15.78	37.34	3.64	13.91	2.86	0.59	2.25	0.39	2.17	0.44	1.29	0.18	1.21	0.18	82.24	12.93	1.02	1.12	1.21
LV55-45	15.93	34.05	3.61	13.56	2.68	0.55	2.22	0.35	1.87	0.37	1.09	0.16	1.03	0.14	77.61	11.33	0.99	1.03	1.45
LV55-48	18.06	39.84	4.09	15.42	3.24	0.62	2.54	0.38	2.11	0.42	1.30	0.17	1.21	0.17	89.58	13.13	0.94	1.06	1.41
Mean	12.84	30.14	3.04	11.84	2.58	0.57	2.22	0.36	2.10	0.43	1.28	0.18	1.22	0.18	68.98	12.49	1.05	1.08	1.05
St. dev.	4.24	9.13	0.89	2.99	0.54	0.10	0.41	0.07	0.41	0.09	0.28	0.04	0.26	0.04	18.19	2.35	0.08	0.07	0.33
Northwestern Pacific																			
LV55-4	6.10	14.30	1.76	7.64	1.89	0.46	1.97	0.34	2.14	0.45	1.39	0.21	1.43	0.22	40.30	12.57	1.04	0.93	0.50
LV71-9	5.89	14.00	1.71	7.87	2.09	0.64	2.24	0.40	2.49	0.54	1.61	0.25	1.66	0.23	41.61	16.70	1.30	0.91	0.43
LV71-10	6.67	15.61	1.83	7.56	1.94	0.58	2.16	0.33	2.00	0.45	1.33	0.19	1.23	0.20	42.10	13.59	1.23	0.98	0.56
1(A1)	14.40	37.10	4.02	16.80	3.85	0.89	4.08	0.60	3.46	0.68	2.17	0.31	2.16	0.33	90.85	16.80	0.98	1.06	0.75
2(A2)	14.00	34.90	3.95	16.30	3.81	0.99	4.18	0.62	3.69	0.89	2.32	0.34	2.40	0.35	88.73	17.90	1.08	1.03	0.68
3(A3)	9.43	22.60	2.85	11.80	2.77	0.74	3.01	0.50	2.86	0.63	1.85	0.27	1.81	0.28	61.40	14.70	1.12	0.95	0.61
4(B1)	10.20	23.90	3.03	12.90	3.07	0.89	3.60	0.57	3.45	0.75	2.22	0.33	2.19	0.33	67.43	17.30	1.16	0.92	0.54
5(B2)	14.10	35.50	3.99	16.00	3.78	0.90	3.98	0.62	3.63	0.77	2.28	0.34	2.36	0.35	88.60	18.20	1.02	1.05	0.68
6(C2)	15.80	39.60	4.31	17.40	4.18	0.97	4.58	0.71	4.21	0.88	2.61	0.39	2.71	0.41	98.77	21.30	0.97	1.06	0.64
7(C1)	13.50	33.50	3.79	16.50	3.88	0.92	4.35	0.67	4.37	0.94	2.85	0.44	3.17	0.49	89.37	24.50	0.98	1.00	0.50
8(D3)	13.30	32.50	3.78	15.40	3.70	0.92	4.10	0.67	4.10	0.89	2.77	0.42	2.84	0.45	85.83	22.30	1.03	1.01	0.53
9(D1)	18.30	45.90	4.83	18.00	4.01	0.95	4.00	0.60	3.38	0.68	2.17	0.30	2.01	0.31	105.4	15.70	1.04	1.13	0.93
11(E1)	15.10	38.00	3.85	14.80	3.26	0.74	3.50	0.51	2.96	0.59	1.84	0.27	1.83	0.28	87.52	14.30	0.95	1.13	0.85
12(E2)	15.00	38.50	3.81	14.80	3.25	0.76	3.46	0.50	3.00	0.60	1.86	0.27	1.83	0.27	87.90	14.10	0.99	1.15	0.84
LV63-3	7.73	17.80	2.53	11.23	2.88	0.90	3.12	0.54	3.29	0.70	2.37	0.30	2.09	0.33	55.81	19.25	1.32	0.84	0.46
LV63-4	10.82	21.01	3.28	12.70	2.98	0.78	3.10	0.51	2.96	0.63	1.76	0.26	1.72	0.26	62.75	15.90	1.12	0.80	0.73
LV63-5	10.29	21.77	3.07	12.68	3.11	0.86	3.11	0.50	3.14	0.65	1.98	0.28	1.88	0.28	63.62	17.71	1.22	0.85	0.63
LV63-8	11.21	24.85	3.24	13.66	3.14	0.87	3.13	0.53	3.19	0.65	1.96	0.28	1.83	0.28	68.83	17.73	1.22	0.89	0.68
LV63-33	8.66	19.32	2.64	11.43	2.84	0.83	2.79	0.47	2.84	0.58	1.74	0.26	1.70	0.25	56.36	16.16	1.29	0.86	0.61
LV63-40	8.39	18.99	2.51	10.32	2.55	0.69	2.52	0.42	2.52	0.53	1.59	0.22	1.53	0.23	53.01	14.27	1.19	0.91	0.64
LV63-44	7.68	17.32	2.42	10.59	2.64	0.82	2.89	0.48	2.98	0.62	1.89	0.27	1.80	0.27	52.68	17.28	1.29	0.85	0.53
Mean	11.27	27.00	3.20	13.16	3.12	0.81	3.33	0.53	3.17	0.67	2.03	0.30	2.01	0.31	70.90	17.06	1.12	0.97	0.63
St. dev.	3.58	9.84	0.88	3.22	0.68	0.14	0.75	0.10	0.62	0.14	0.41	0.07	0.48	0.07	20.09	2.96	0.12	0.11	0.13
Bering Sea																			
LV63-9	7.71	16.98	2.24	9.18	2.11	0.59	2.04	0.34	1.94	0.39	1.20	0.18	1.22	0.18	46.29	10.85	1.24	0.90	0.74
LV63-12	13.10	27.85	3.45	13.16	2.83	0.68	2.61	0.42	2.42	0.49	1.47	0.22	1.48	0.23	70.41	13.40	1.11	0.94	0.92
LV63-15	15.13	31.28	3.88	14.77	3.20	0.85	2.82	0.44	2.70	0.50	1.51	0.21	1.36	0.21	78.84	13.91	1.23	0.93	1.10
LV63-20	19.71	39.96	4.89	18.57	3.69	0.89	3.43	0.50	2.61	0.50	1.53	0.21	1.35	0.21	98.06	14.15	1.10	0.93	1.39
LV63-23	18.93	38.41	4.73	17.53	3.57	0.79	3.03	0.46	2.54	0.48	1.45	0.19	1.27	0.19	93.58	13.23	1.06	0.94	1.43
Mean	14.92	30.89	3.84	14.64	3.08	0.76	2.79	0.43	2.44	0.47	1.43	0.20	1.34	0.20	77.44	13.10	1.15	0.93	1.12
St. dev.	4.86	9.24	1.08	3.73	0.64	0.12	0.51	0.06	0.30	0.05	0.14	0.02	0.10	0.02	20.66	1.32	0.08	0.02	0.30

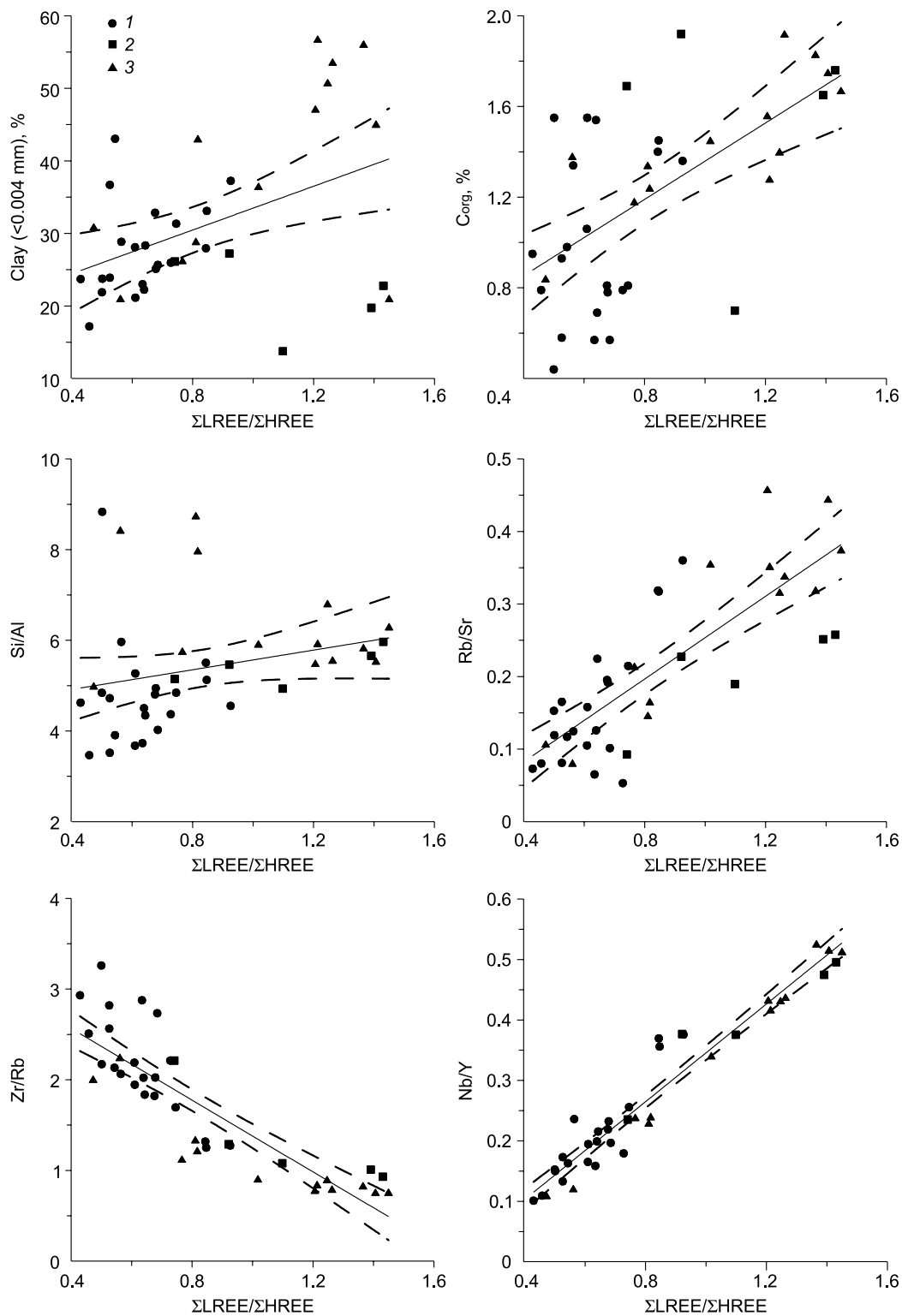


Fig. 3. Ratios between $\Sigma\text{LREE}/\Sigma\text{HREE}$ and clay fraction, C_{org} and Si/Al, Rb/Sr, Zr/Rb, Nb/Y in the surface bottom sediments of the Northwestern Pacific. 1, Pacific Ocean; 2, Bering Sea; 3, Sea of Okhotsk. The thin line is the regression line (trend), the dashed line is the confidence interval (95%) for the regression line, i.e., the regression line passes between the two dashed curves with a 95% probability.

the second important source of clastic matter in the bottom sediments of the Northwestern Pacific after river discharge, abrasion and ice rafting (Dergachev and Nikolaeva, 2010).

Two groups of stations were distinguished using cluster analysis (Fig. 4) and carried out according to a successive merging graph. Cluster I includes the stations are located on

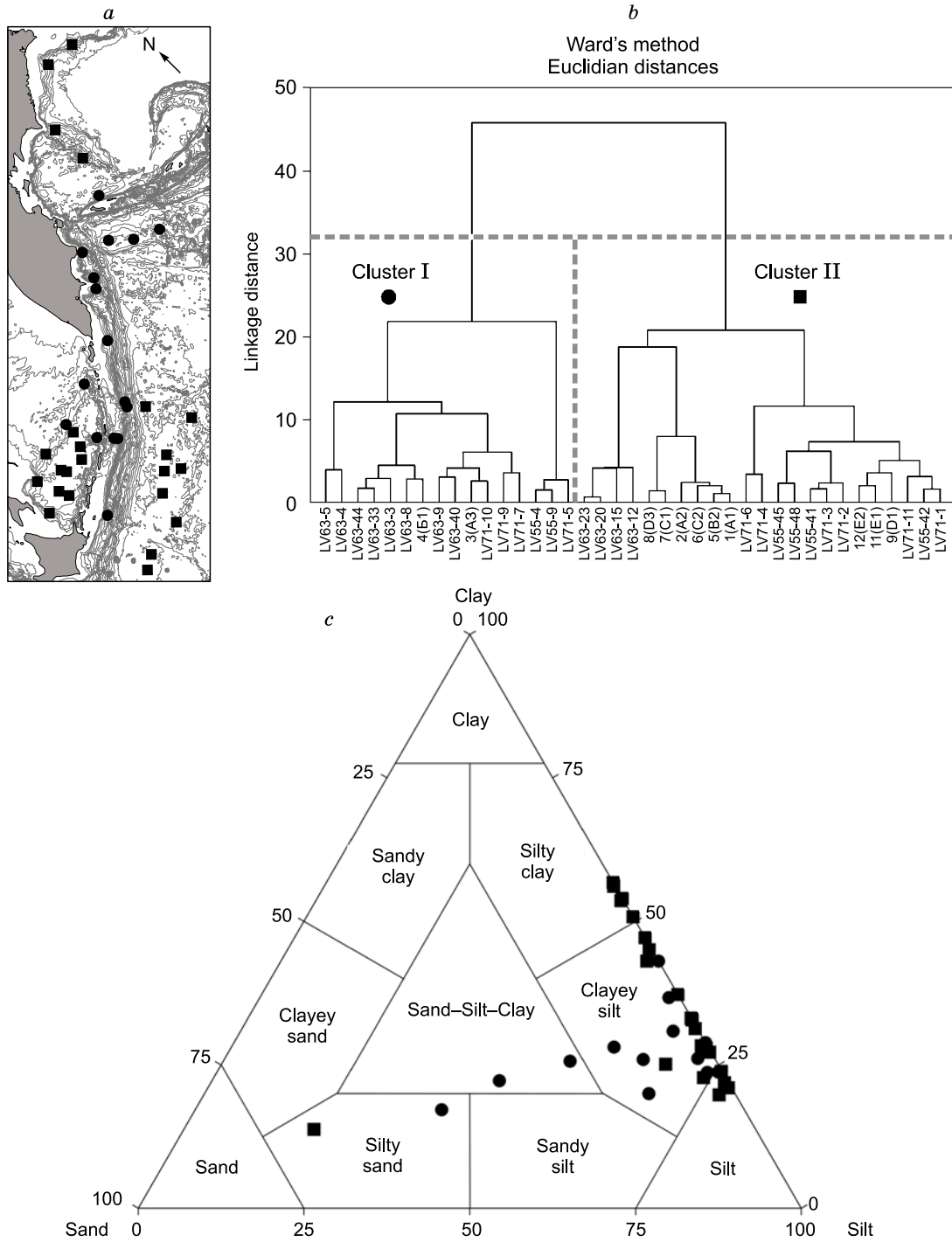


Fig. 4. The results of statistical data processing. *a*, Location of sampling station (circles, cluster I, squares, cluster II); *b*, cluster analysis dendrogram; *c*, Shepard's classification diagram.

the sloped or submarine hills along the Kuril Islands, Kamchatka, and the Commander Islands (Fig. 4). LREE enrichment can be explained by additional sorption of light rare earths because in the other samples whose grain composition is close to silt this correlation almost disappears. Possibly, this is due to of distributive provinces and lithodynamic environment. For that reason, we performed a cluster

analysis for geochemical typification of the studied bottom sediments.

Two groups of stations were distinguished using cluster analysis (Fig. 4) and carried out according to a successive merging graph. Cluster I includes the stations are located on the sloped or submarine hills along the Kuril Islands, Kamchatka, and the Commander Islands (Fig. 4). The station

Table 4. Comparison of the REE concentration average values for the distinguished clusters (the units correspond to those in Tables 2 and 3)

	Si	Al	Fe	Mn	Ca	Ti	Mg	K	Li	Nb	Cs	Cr	Hf	Th	U	Sc	Pb	Rb	Sr	Zn	Zr	P3Э	Y
Cluster I																							
Mean	28	5.9	3.7	0.24	3.5	0.31	1.52	1.06	18	2.47	1.82	42	1.72	1.87	0.96	16	11	28	295	86	63	53	15
St. dev.	2	1.5	1.0	0.4	2.5	0.09	0.33	0.21	5	0.59	0.39	22	0.49	0.49	0.23	5	3	6	100	13	15	11	3
Cluster II																							
Mean	29	5.4	3.1	0.84	1.3	0.25	1.23	1.42	29	5.00	4.06	43	2.28	4.23	1.45	12	20	58	215	98	71	84	15
St. dev.	2	0.8	0.3	1.1	0.5	0.04	0.17	0.20	7	1.10	0.93	19	1.13	1.60	0.24	2	7	13	31	19	22	12	4
	La	Ce	Pr	Nd	Sm	Eu	Gd	Tb	Dy	Ho	Er	Tm	Yb	Lu	Eu/Eu*	Ce/Ce*	(LnL/LnH) _N						
Cluster I																							
Mean	8.18	18.68	2.40	10.16	2.49	0.70	2.58	0.43	2.62	0.55	1.68	0.24	1.61	0.24	1.20	0.92	0.59						
St. dev.	1.85	3.76	0.60	2.38	0.55	0.17	0.64	0.10	0.62	0.13	0.41	0.06	0.38	0.06	0.08	0.09	0.11						
Cluster II																							
Mean	15.09	35.41	3.80	14.82	3.25	0.74	3.10	0.48	2.80	0.57	1.72	0.25	1.69	0.25	1.03	1.06	1.00						
St. dev.	2.37	4.94	0.60	2.26	0.55	0.16	0.85	0.12	0.79	0.19	0.55	0.09	0.63	0.10	0.07	0.07	0.31						

LV71-5 is only remote and locate on the northeastern slope of the Kuril Basin. The other stations were grouped in cluster II. The differential characteristic of the clusters is differences in concentration of some elements as a synchronous increase in concentration of Mn, Nb, Cs, Th, U, Pb, Rb and LREE (Table 4). At the same time, the average values of HREE concentrations remained similar between the clusters. The clusters have no almost no dissimilarity in organic carbon concentrations. The average C_{org} contents in cluster I and cluster II are 1.1 and 1.3%, respectively. The cluster I samples contained higher sandy fraction than samples from cluster II. At the same time, the silty fraction (0.004–0.063 mm) is almost identical in the both groups (about 60%). Cluster II was also characterized by an increased clayey fraction.

The cluster I samples have a LREE/HREE ratio of less than 1 varying from 0.43 to 0.81. The REE spectra of cluster I almost repeated the spectra for the volcanic rocks of the Kuril Islands and Kamchatka Peninsula (Hochstaedter et al., 1996; Martynov et al., 2010). The same can be said about the Geophysicist Seamount (Baranov et al., 2002), which is a sign of the effect of edaphogenic material on REE composition in the bottom sediments of the considered cluster. Also, the coincidence of the REE spectra is observed with the suspensions of the Kislaya River on Kunashir Island (Chudaeva and Chudayev, 2011) and approximately similar to the REE spectra of river sediments from Hokkaido Island (Ohta et al., 2007). In general, the chemical composition of the bottom sediments of the Kuril–Kamchatka arc is close to the volcanic rocks of the distributive provinces (Astakhov, 2001).

Cluster II have a diverse REE spectrum including samples whose LREE/HREE ratios were both higher and lower than 1 (Fig. 2). The lanthanides spectra are comparable to those from the distributive provinces. Terrigenous material is brought to the Bering Sea mainly by the discharge of big rivers—the Anadyr, Yukon and Kuskokwim that drain two-

thirds of the sea's catchment area. The solid discharge of small rivers and marine erosion are of secondary importance (Lisytsyn, 1966). The sediments of the northwestern part of the Bering Sea including the stations on Shirshov Ridge in their normalized lanthanides distribution are similar to those from the Anadyr Gulf (Anikiev et al., 1997), where sedimentation is mainly affected by the discharge of the Anadyr River, transported by the western branch of the cyclonic surface-water circulation formed by ice rafting. At the same time, REE concentration in Kuril Basin sediments is comparable to the one in the sediments of the northwestern Sea of Okhotsk (Sattarova et al., 2014) and the Amur River (Sorokina and Zarubina, 2011). For that reason, it is possible that terrigenous material from the Amur River could reach the deep-water parts of the Sea of Okhotsk by means of suspension transition along the east coast of Sakhalin Island as well as by drifting ice (Zou et al., 2015). REE concentration in the bottom sediments of the Pacific pelagic region is also affected by atmospheric drift, mostly dust transfer from East Asian deserts and volcanic eruptions of the Pacific Ring of Fire (Ziegler et al., 2007). In the abyssal part of the Pacific the enrichment of silt by the amorphous silica is related to the presence of huge amounts of organisms with opaline skeletons such as diatoms and deep-water sponges, which confirms the high biological productivity of surface oceanic waters. On the other hand, presence of biogenic silica in sediments significantly reduces REE concentration (Palmer, 1985). According to (Akagi et al., 2011) diatoms are important bearers of heavy REE.

CONCLUSIONS

The REE concentration in the bottom sediments from the Northwestern Pacific varies from 30 to 106 ppm, yttrium concentration ranges from 9.34 to 24.5 ppm, which is significantly less than in deep-water clays of the central part of the Pacific.

The changes in the total REE concentration are mainly due to LREE. Heavy lanthanides, on the other hand, do not change that much. The sediments containing coarse fractions have a negative Ce anomaly that becomes positive in fine fractions.

The bottom sediments in the Kuril–Kamchatka arc area are not that rich in REE if compared to the sediments of the abyssal plane of the Pacific, the Kuril basin and the northwestern part of the Bering Sea. The rare-earth elements concentration and fractioning is determined by the effect of distributive provinces and lithodynamic (geodynamic and hydrological) environment of the region that is manifested in the positive correlation with the LREE/HREE ratio, the grain composition, the Rb/Sr, Nb/Y values, and in the negative correlation with the Zr/Rb values.

Considering their chemical composition, the studied samples can be divided into two clusters. The first cluster includes the Kuril–Kamchatka province. Here, the supply of the clastic matter and its redistribution is determined by the relief and the main water currents. For that reason, heavy rare earths rarely reach deep-water areas, where mainly terrigenous and biogenic-terrigenous silts are accumulated that comprise cluster II.

The authors are grateful to the researchers of the Laboratory of Geochemical Processes POI FEB RAS, Prof. Dr. A. Brandt (Senckenberg Research Institute and Natural History Museum, Germany), Dr. M.V. Malyutina (National Science Center of Marine Biology FEB RAS), and Dr. S.A. Gorbarenko (V.I. Il'ichev Pacific Oceanological Institute FEB RAS) for an invitation to join the expedition. Thanks are due to the Captain and crew of the RV “Akademik M.A. Lavrent'ev” and RV “Sonne” for their help with the sampling. Special thanks go to the Laboratory of Analytical Chemistry at the Far East Geological Institute for help with chemical analyses. We are also very grateful to anonymous reviewers of our manuscript for their valuable comments and suggestions, which greatly improved this document.

The work was supported by the Russian Foundation for Basic Research (grant No. 16-04-01431-a), by the National Natural Science Foundation of China (U160641, 41420104005) and by the State theme “Paleoceanology of marginal seas of Eastern Russia and adjacent regions of the Pacific Ocean, features and stages of Cenozoic sedimentation, magmatism and ore genesis” (No. AAAA-A17-117030110033-0).

REFERENCES

- Akagi, T., Fu, F.-fu., Hongo, Y., Takahashi, K., 2011. Composition of rare earth elements in settling particles collected in the highly productive North Pacific Ocean and Bering Sea: Implications for siliceous-matter dissolution kinetics and formation of two REE-enriched phases. *Geochim. Cosmochim. Acta* 75 (17), 4857–4876.
- Anikiev, V.V., Dudarev, O.V., Botsul, A.I., Kolesov, G.M., Sapozhnikov, D.Yu., 1997. Distribution and sedimentation fluxes of chemical elements in the particulate matter-bottom sediments system at the transition from the Anadyr river estuary to the Bering sea. *Geochem. Int.* 35 (3), 274–283.
- Anikiev, V.V., Dudarev, O.V., Kolesov, G.M., Botsul, A.I., Sapozhnikov, D.Yu., 1997. Distribution and sedimentation flow of chemical elements in the system suspension—bottom sediments of Anadyr River–Bering Sea estuary. *Geokhimiya*, No. 3, 320–330.
- Astakhov, A.S., 2001. Lithochemistry of the Continental Sediments of Eastern Asia [in Russian]. Dal'nauka, Vladivostok.
- Bailey, J.C., 1993. Geochemical history of sediments in the northwestern Pacific Ocean. *Geochem. J.* 27, 71–90.
- Balashov, Yu.A., 1976. Rare Earth Geochemistry [in Russian]. Nauka, Moscow.
- Baranov, B.V., Werner, R., Hoernle, K.A., Tsoy, I.B., Van Den Bogaard, P., Tararin, I.A., 2002. Evidence for compressionally induced high subsidence rates in the Kurile basin (Sea of Okhotsk). *Tectonophysics* 350 (1), 63–97.
- Baturin, G.N., Yushina, I.G., 2007. Rare earth elements in phosphate-ferromanganese crusts on Pacific seamounts. *Lithol. Min. Resour.* 42 (2), 101–117.
- Belousov, V.V., Udintsev, G.B., (Eds.), 1981. Sea of Okhotsk Bottom Structure [in Russian]. Nauka, Moscow, 1981.
- Bezrukov, P.L., 1955. Bottom sediments of the Kuril–Kamchatka basin, in: *Trans. Oceanology Institute*, Issue 12 [in Russian]. Izd. AN SSR, Moscow, pp. 97–129.
- Botsul, A.I., 2002. The Analysette 22 laser particle size measurer: advantages, problems and some particularities of utilization when analyzing bottom sediments, in: *Conditions of Formation of Bottom Sediments and Related Minerals in Marginal Seas* [in Russian]. Dal'nauka, Vladivostok, pp. 114–118.
- Chudaeva, V.A., Chudaev, O.V., 2011. Accumulation and fractioning of rare earth in the Far-East surface waters in presence of natural and anthropogenic anomalies. *Geochem. Int.* 5, 523–549.
- Dergachev, A.N., Nikolaeva, N.A., 2010. Mineralogical Indicators of Near-Continental Sedimentation in Western Pacific [in Russian]. Dal'nauka, Vladivostok.
- Dou, Y.G., Yang, S.Y., Liu, Z.X., Clift, P.D., Shi, X.F., Yu, H., Berne, S., 2010. Provenance discrimination of siliciclastic sediments in the middle Okinawa Trough since 30 ka: Constraints from rare earth element compositions. *Mar. Geol.* 275, 212–220.
- Dubinin, A.V., 1994. Rare earth geochemistry in the sediments and concretions of the Pacific Guatemala basin: effect of early diagenesis. *Geokhimiya*, No. 8/9, 1335–1345.
- Dubinin, A.V., 1998a. Rare-earth elements in early diagenesis processes in the Pacific. *Litologiya i Poleznye Iskopaemye*, No. 4, 762–772.
- Dubinin, A.V., 2006. Geochemistry of Oceanic Rare Earth Elements [in Russian]. Nauka, Moscow.
- Dubinin, A.V., Sval'nov V.N., 2001. Sedimentation evolution from studying autogenic and biogenic phases in the pelagic sediments of the South Basin of the Pacific. *Geokhimiya*, No. 4, 404–421.
- Dubinin, A.V., Sval'nov, V.N., 2003. Geochemistry of the manganese ore process in the ocean: evidence from rare earth elements. *Lithol. Min. Resour.* 38 (2), 91–100.
- Dubinin, A.V., Volkov, I.I., 1986. Rare earth elements in the metal-bearing sediments of the East Pacific Elevation. *Geokhimiya*, No. 5, 645–662.
- Dubinin, A.V., Sval'nov, V.N., Berezhnaya, E.D., Rimskaya-Korsakova, M.N., Demidova, T.P., 2013. Geochemistry of trace and minor elements in sediments and manganese micronodules from the Angola Basin. *Lithol. Min. Resour.* 48 (3), 175–197.
- Gromet, L.P., Dymek, R.F., Haskin, L.A., Korotev, R.L., 1984. The “North American Shale Composite”. Its Compilation, Major and Trace Element Characteristics. *Geochim. Cosmochim. Acta* 48, 2469–2482.
- Gurvich, E.G., Lukashin, V.N., Lisitsyn, A.P., Kurinov, A.D., 1980. Rare earth elements and yttrium, in: *Ronova A.B. (Ed.), Geochemistry of Hydrolysates* [in Russian]. Nauka, Moscow, pp. 71–116.
- Henderson, P., 1984. Rare Earth Element Geochemistry. Oxford, Elsevier.

- Hochstaedter, A.G., Kepezhinskas, P., Defant, M., Drummond, M., Koleskov, A., 1996. Insights into the volcanic arc mantle wedge from magnesian lavas from the Kamchatka arc. *J. Geophys. Res. Solid Earth* 101 (B1), 697–712.
- Kato, Y., Fujinaga, K., Nakamura, K., Takaya, Y., Kitamura, K., Ohta, J., Toda, R., Nakashima, T., Iwamori, H., 2011. Deep-sea mud in the Pacific Ocean as a potential resource for rare-earth elements. *Nat. Geosci.* 4, 535–539.
- Li, Y.-H., 1982. Interelement relationship in abyssal Pacific ferromanganese nodules and associated pelagic sediments. *Geochim. Cosmochim. Acta* 46 (6), 1053–1060.
- Lisysyn, A.P., 1966. Modern-Day Sedimentation in the Bering Sea [in Russian]. Nauka, Moscow.
- Martynov, Y.A., Khanchuk, A.I., Kimura, D.-I., Rybin, A.V., Martynov, A.Yu., 2010. Geochemistry and petrogenesis of the Quaternary volcanites of the Kuril Island arc. *Petrology* 18 (5), 512–535.
- Mazarovich, A.O., 2011. Marginal seas—Terminological crisis. *Geotectonics* 45: 317, 60–78.
- Murray, R.W., Buchhiltz ten Brink, M.R., Brumsack, H.J., Gerlach, D.C., Price Russ, G., 1991. Rare-earth elements in Japan Sea sediments and diagenetic behavior of Ce/Ce*: Results from ODP Leg 127. *Geochim. Cosmochim. Acta* 55, 2453–2466.
- Ohta, A., Imai, N., Terashima, S., Tachibana, Y., 2007. Elemental distribution of coastal sea and stream sediments in the island-arc region of Japan and mass transfer processes from terrestrial to marine environments. *Appl. Geochem.* 22 (12), 2872–2891.
- Otosaka, S., Noriki, S., 2000. REEs and Mn/Al ratio of settling particles: horizontal transport of particulate material in the northern Japan Trench. *Mar. Chem.* 72, 329–342.
- Palmer, M.R., 1985. Rare-earth elements in foraminifera tests. *Earth Planet. Sci. Lett.* 73, 285–298.
- Rodnikov, A.G., Zabarinskaya, L.P., Pi'p, V.B., Rashidov, V.A., Sergeeva, N.A., Filatova, N.I., 2005. Sea of Okhotsk geotraverse. *Vestnik KRAUNTS. Earth Sci. Ser.* 5, 45–58.
- Rogachev, K.A., Verkhunov, A.V., 1995. Circulation and water mass structure in the southern Sea of Okhotsk, as observed in summer 1994, in: *Proc. Workshop on the Sea of Okhotsk and Adjacent Areas, PICES Sci. Rep.*, Vol. 6, pp. 144–149.
- Sattarova, V.V., Artemova, A.V., 2015. Geochemical and micropaleontological character of deep-sea sediments from the northwestern Pacific near the Kuril–Kamchatka Trench, in: *Deep Sea Research. Pt. II: Topical Studies in Oceanography*, Vol. 111, pp. 10–18.
- Sattarova, V.V., Zarubina, N.V., Blokhin, M.G., Mariash, A.A., 2014. Rare-earth in the surface sediments of the Derugin Trench of the Sea of Okhotsk. *Pacific Geol.* 33 (2), 109–117.
- Sorokina, O.A., Zarubina, N.V., 2011. Sediments chemical composition in the mid-stream of the Amur River. *Pacific Geol.* 30 (5), 105–113.
- Soyol-Erdene, T.O., Huh, Y., 2013. Rare earth element cycling in the pore waters of the Bering Sea Slope (IODP Exp. 323). *Chem. Geol.* 358, 75–89.
- Sterkopaytov, S.V., Dubinin, A.V., 1996. Rare earth elements as indicators for oceanic distributive province composition (exemplified by Pacific profile). *Litologiya i Poleznye Iskopaemye*, No. 4, 438–444.
- Taylor, S.R., McLennan, S.M., 1985. *The Continental Crust: Its Composition and Evolution; an Examination of the Geochemical Record Preserved in Sedimentary Rocks*. Blackwell, Oxford.
- Tlig, S., Steinberg, M., 1982. Distribution of rare-earth elements (REE) in size fractions of recent sediments of the Indian Ocean. *Chem. Geol.* 37, 317–333.
- Toyoda, K., Nakamura, Y., Masuda, A., 1990. Rare earth elements of Pacific pelagic sediments. *Geochim. Cosmochim. Acta* 54, 1093–1103.
- Udintsev, G.B., 1955. The Kuril–Kamchatka Trench's Relief, in: *Trans. Oceanology Institute, Issue 12* [in Russian]. Isd. AN SSSR, Moscow, pp. 97–129.
- Vasil'ev, B.I., Tatarin, I.A., Govorov, I.N., Konovalov Yu.I., 1986. New data on the geological composition of the Kuril–Kamchatka Trench. *Tikhookeanskaya Geologiya*, No. 3, 64–73.
- Volkov, I.I., Fomina, L.S., 1973. New data on the geochemistry of rare-earth elements in the sediments of the Pacific Ocean. *Geokhimiya*, No. 11, 1603–1615.
- Zhang, X., Zhang, F., Chen, X., Zhang, W., Deng, H., 2012. REEs fractionation and sedimentary implication in surface sediments from eastern South China Sea. *J. Rare Earth* 30 (6), 614–620.
- Ziegler, C.L., Murray, R.W., Hovan, S.A., Rea, D.K., 2007. Resolving eolian, volcanogenic, and authigenic components in pelagic sediment from the Pacific Ocean. *Earth Planet. Sci. Lett.* 254, 416–432.
- Zou, J., Shi, X., Zhu, A., Chen, M.-T., Kao, S., Wu, Y., Selvaraj, K., Scholz, P., Bai, Y., Wang, K., Ge, S., 2015. Evidence of sea ice-driven terrigenous detritus accumulation and deep ventilation changes in the southern Sea of Okhotsk during the last 180 ka. *J. Asian Earth Sci.* 114, 541–548.

Editorial responsibility: A.E. Isokh